Inorg. Chem. **2006**, *45*, 10108–10114

Kinetics and Mechanism of the Oxidation of Guanosine Derivatives by Pt(IV) Complexes

Sunhee Choi,* Livia Vastag, Chin-Hin Leung, Adam M. Beard, Darcy E. Knowles, and James A. Larrabee

Department of Chemistry and Biochemistry, Middlebury College, Middlebury, Vermont 05753

Received July 5, 2006

The kinetics of redox reactions of the Pt^{IV} complexes *trans*-Pt(*d,l*)(1,2-$(NH_2)_2C_6H_{10}$)Cl_4 ([$Pt^{IV}Cl_4$(dach)]) and Pt(NH_2-$CH_2CH_2NH_2$)Cl_4 ([$Pt^{IV}Cl_4$(en)]) with 5′- and 3′-dGMP (G) have been studied. These redox reactions involve substitution followed by an inner-sphere electron transfer. The substitution is catalyzed by Pt^{II} and follows the classic Basolo–Pearson Pt^{II}-catalyzed Pt^{IV}-substitution mechanism. We found that the substitutution rates depend on the steric hindrance of Pt^{II}, G, and Pt^{IV} with the least sterically hindered Pt^{II} complex catalyzing at the highest rate. 3′-dGMP undergoes substitution faster than 5′-dGMP, and [$Pt^{IV}Cl_4$(en)] substitutes faster than [$Pt^{IV}Cl_4$(dach)]. The enthalpies of activation of the substitution, $\Delta H_s^{\ddagger}$, of 3′-dGMP is only 70% greater than that of 5′-dGMP (50.4 vs 30.7 kJ mol^{-1}), but the entropy of activation of the substitution, $\Delta S_s^{\ddagger}$, of 3′-dGMP is much greater than that of 5′-dGMP (–59.4 vs –129.5 J K^{-1} mol^{-1}), indicating that steric hindrance plays a major role in the substitution. The enthalpy of activation of electron transfer, $\Delta H_e^{\ddagger}$, of 3′-dGMP is smaller than that of 5′-dGMP (88.8 vs 137.8 kJ mol^{-1}). The entropy of activation of electron transfer, $\Delta S_e^{\ddagger}$, of 3′-dGMP is negative, but that of 5′-dGMP is positive (–27.8 vs +128.8 J K^{-1} mol^{-1}). The results indicate that 5′-hydroxo has less rotational barrier than 5′-phosphate, but it is geometrically unfavorable for internal electron transfer. The electron-transfer rate also depends on the reduction potential of Pt^{IV}. Because of its higher reduction potential, [$Pt^{IV}Cl_4$(dach)] has a faster electron transfer than [Pt^{IV}-Cl_4(en)].

Introduction

Platinum complexes are biologically important because of their anticancer activities. In particular, the interaction of DNA with Pt^{II} complexes has been extensively studied.[1] On the other hand Pt^{IV} complexes, which are relatively inert, have not been the focus of much research because potential reactivity with DNA is not generally expected for such inert molecules. However, our lab recently discovered that *trans*-Pt(*d,l*)(1,2-$(NH_2)_2C_6H_{10}$)Cl_4, [$Pt^{IV}Cl_4$(dach)], oxidizes 5′-dGMP, 3′-dGMP, and 5′-d[GTTTT]-3′.[2] The proposed mechanism involves Pt^{IV} binding to N7 of the guanosine (G) moiety followed by nucleophilic attack of a 5′-phosphate or a 5′-hydroxyl oxygen to C8 of the G moiety and an inner-sphere, two-electron transfer to produce cyclic (5′-O-C8)-G and a Pt^{II} complex (Scheme 1). The identity of the final oxidized G depends on the hydrolysis rate of the cyclic intermediate. The cyclic phosphodiester intermediate formed from [$Pt^{IV}Cl_4$(dach)]/5′-dGMP is hydrolyzed to 8-oxo-5′-dGMP. However the cyclic ether intermediate formed from [$Pt^{IV}Cl_4$(dach)]/3′-dGMP (or 5′-d[GTTTT]) does not hydrolyze, and this cyclic form is the final oxidation product. The Pt^{IV} complex simply binds to N7 of the G moiety in 3′,5′-cyclic guanosinemonophosphate (cGMP), 9-methylxanthine (9-Mxan), 5′-d[TTGTT]-3′, and 5′-d[TTTTG]-3′ without further redox reaction. These prior results indicate that a

* To whom correspondence should be addressed. E-mail: choi@middlebury.edu.

(1) (a) Fuertes, M. A.; Alonso, C.; Perez, J. M. *Chem. Rev.* **2003**, *103*, 645−662. (b) Lippert, B. *Cisplatin: Chemistry and Biochemistry of a Leading Anticancer Drug*; Wiley-VCH: Weinheim, Germany, 1999. (c) Hartley, F. R. *Chemistry of the Platinum Group Metals, Recent Developments*; Elsevier: Amsterdam, 1993. (d) Hall, M. D.; Hambley, T. W. *Coor. Chem. Rev.* **2002**, *232*, 49−67.

(2) (a) Choi, S.; Cooley, R. B.; Voutchkova, A.; Leung, C. H.; Vastag, L.; Knowles, D. E. *J. Am. Chem. Soc.* **2005**, *127*, 1773−1781. (b) Choi, S.; Cooley, R. B.; Hakemian, A. S.; Larrabee, Y. C.; Bunt, R. C.; Maupaus, S. D.; Muller, J. G.; Burrows, C. J. *J. Am. Chem. Soc.* **2004**, *126*, 591−598. (c) Choi, S.; Delaney, S.; Orbai, L.; Padgett, E. J.; Hakemian, A. S. *Inorg. Chem.* **2001**, *40*, 5481−5482. (d) Choi, S.; Mahalingaiah, S.; Delaney, S.; Neale, N. R.; Masood, S. *Inorg. Chem.* **1999**, *38*, 1800−1805. (e) Choi, S.; Filotto, C.; Bisanzo, M.; Delaney, S.; Lagasee, D.; Whitworth, J. L.; Jusko, A.; Li, C.; Wood, N. A.; Willingham, J.; Schwenker, A.; Spaulding, K. *Inorg. Chem.* **1998**, *37*, 2500−2504.

10.1021/ic061243g CCC: $33.50 © 2006 American Chemical Society
Published on Web 11/15/2006

Scheme 1. Proposed Mechanism for the Reaction of $[Pt^{IV}Cl_4(dach)]$ with 5′-dGMP, 3′-dGMP, and cGMP[2a,b]

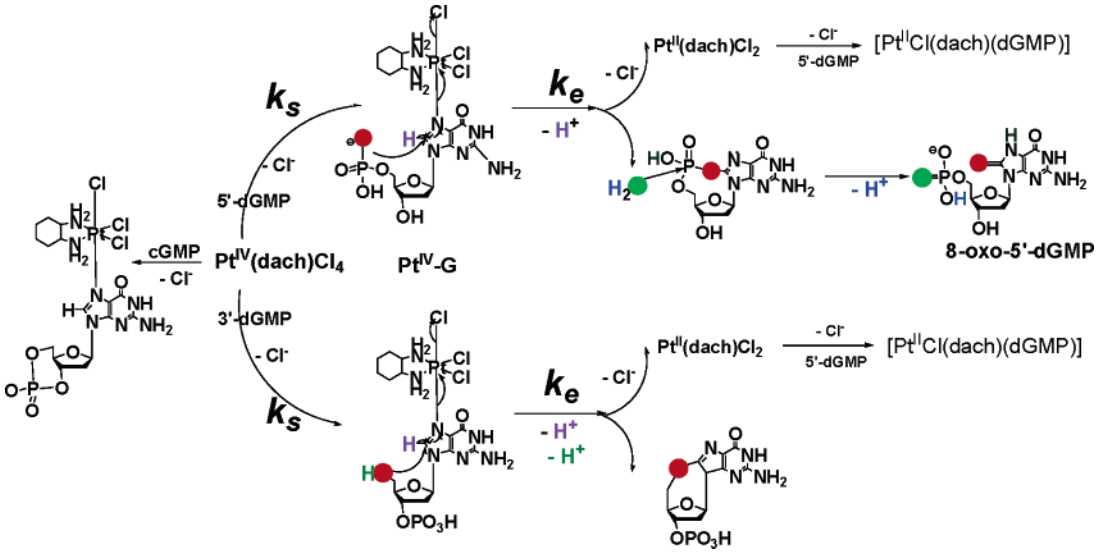

nucleophilic group at the 5′ position is required for the redox reaction between G and the Pt^{IV} complex.

Although the kinetics of Pt^{II} complex binding to DNA is fairly well understood,[3,4] the corresponding Pt^{IV} chemistry is not. Roat and co-workers reported that the reaction of several Pt^{IV} complexes with 9-Mxan undergo Pt^{II}-catalyzed Pt^{IV} substitution reactions without autocatalysis, where the added Pt^{II} catalysts were Pt^{IV} analogues.[5] Elding's group established a redox mechanism for reductive elimination at Pt^{IV} where two electrons transfer between the reductant (thiol or ascorbate) and the Pt^{IV} via a halide ligand.[6] Several other groups reported the autocatalytic nature of Pt^{IV} reduction by ascorbate via an outer-sphere, as well as an inner-sphere, one-electron transfer.[7] None of these cases have a mechanism similar to the $[Pt^{IV}Cl_4(dach)]$/dGMP redox reaction, where substitution precedes inner-sphere two-electron transfer.[2a,b]

In our previous work,[2a] we observed that 3′- and 5′-dGMP reactions with $[Pt^{IV}Cl_4(dach)]$ were autocatalyzed, and 3′-dGMP reacted faster than 5′-dGMP. The aim of the present work is to expand on our earlier studies of the substitution and electron-transfer mechanism using quantitative kinetic measurements. Using an autocatalytic kinetic model and the DynaFit Software,[8] we obtained the substitution rate constant (k_s) and the electron-transfer rate constant (k_e). Activation parameters were obtained from the rate constants at temperatures between 30 and 45 °C. We also compared the $[Pt^{IV}Cl_4(dach)]$ reaction rates to $[Pt^{IV}Cl_4(en)]$ to see how the size of the carrier ligand and the reduction potential of Pt^{IV} complexes affect substitution and electron-transfer rates. To the best of our knowledge, this is the first detailed kinetic study of a Pt^{IV}/DNA reaction.

Experimental Section

Sample Preparation. $[Pt^{IV}Cl_4(dach)]$ was obtained from the National Cancer Institute, Drug Synthesis and Chemistry Branch, Developmental Therapeutics Program, Division of Cancer Treatment. The $[Pt^{II}Cl_2(diam)]$ and $[Pt^{II}(tetam)]$ complexes were purchased from Sigma Aldrich. $[Pt^{II}Cl_2(dach)]$,[9a] $[Pt^{II}Cl_2(en)]$,[9b] and $[Pt^{IV}Cl_4(en)]$[9b] were synthesized following previously published procedures. They were characterized by IR (Bruker Equinox 55 Spectrometer), ^{1}H NMR (Bruker 400 Ultrashield spectrometer), and HPLC (Waters Alliance 2695 equipped with a Waters 2996 Photodiode Array Detector and a Waters Atlantis dC18 column). $[Pt^{II}Cl(dach)(5'\text{-dGMP})]$ and $[Pt^{II}(diam)(5'\text{-dGMP})_2]$ were synthesized by the reactions of 5′-dGMP with stoichiometric amounts of $[Pt^{II}Cl_2(dach)]$ and $[Pt^{II}Cl_2(diam)]$, respectively. Stock platinum complex solutions were prepared by dissolution in saline water (0.1 M NaCl, pH 8.3−8.6). pH 8.3−8.6 was used to fully deprotonate the phosphate group in dGMP,[10] and a 0.1 M NaCl solution was used to prevent hydrolysis of the platinum complexes.

Mass Spectrometry. Liquid chromatography/mass spectrometry (LC/MS) analyses were conducted on an 1100 Series LC and LC/MSD Trap XCT Plus from Agilent Technologies. The LC component was equipped with a photodiode array detector and an Eclipse X-D8-C8 column (5 μm, 4.6 × 150 mm) under isocratic

(3) (a) Bancroft, D. P.; Lepre, C. A.; Lippard, S. J. *J. Am. Chem. Soc.* **1990**, *112*, 6860−6871. (b) McGowan, G.; Parsons, S.; Sadler, P. *Inorg. Chem.* **2005**, *44*, 7459−7467. (c) Arpalahti, J.; Lippert, B. *Inorg. Chem.* **1990**, *29*, 104−110.
(4) (a) van Eldik, R.; Palmer, D. A.; Kelm, H. *Inorg. Chem.* **1979**, *18*, 572−577. (b) Inagaki, K.; Dijit, F. J.; Lempers, E. L. M.; Reedijk, J. *Inorg. Chem.* **1988**, *27*, 382−387. (c) Summa, N.; Schiessl, W.; Puchta, R.; van Eikema Hommes, N. ; van Eldik, R. *Inorg. Chem.* **2006**, *45*, 2948−2959. (d) Wong, H. C.; Coogab, R.; Intini, F. P.; Natile, G.; Marzilli, L. *Inorg. Chem.* **1999**, *38*, 777−787. (e) Schmulling, M.; Lippert, B.; van Eldik, R. *Inorg. Chem.* **33**, 3276−3280. (f) Kasparkova, J.; Marini, V.; Najajreh, Y.; Gibson, D.; Brabec, V. *Biochemistry* **2003**, *42*, 6321−32. (g) Williams, K. M.; Rowan, C.; Mitchell, J. *Inorg. Chem.* **2004**, *43*, 1190−1196.
(5) Roat, R. M.; Jerardi, M. J.; Kopay, C. B.; Heat, D. C.; Clark, J. A.; DeMars, J. A.; Weaver, J. M.; Bezemer, E.; Reedijk, J. *J. Chem. Soc., Dalton Trans.* **1997**, 3615−3621.
(6) (a) Lemma, K.; Shi, T.; Elding, L. I. *Inorg. Chem.* **2000**, *39*, 1728−1734. (b) Lemma, K.; Sargeson, A. M.; Elding, L. I. *J. Chem. Soc., Dalton Trans.* **2000**, 1167−1172. (c) Lemma, K.; Berglund, J.; Farrell, N.; Elding, L. I. *J. Biol. Inorg. Chem.* **2000**, *5*, 300−306.
(7) (a) Weaver, E. L.; Bose, R. N. *J. Inorg. Biochem.* **2003**, 95, 231−239. (b) Bose, R. N.; Weaver, E. L. *J. Chem. Soc., Dalton Trans.* **1997**, 1797−1799. (c) Evans, D. J.; Green, M. *Inorg. Chim. Acta*. **1987**, 183−185.
(8) Kuzmic, P. *Anal. Biochem.* **1996**, *237*, 260−273.
(9) (a) Blatter, E. E.; Vollano, J. F.; Krishna, B. S.; Babrowiak, J. C. *Biochemistry* **1984**, *21*, 4817−4820. (b) Ellis, L. T.; Er, H. M.; Hambley, T. W. *Aust. J. Chem.* **1995**, *48*, 793−806.
(10) Berbeners-Price, S. J.; Frey, U.; Ranford, J. D.; Sadler, P. J. *J. Am. Chem. Soc.* **1993**, *115*, 8649−8659.

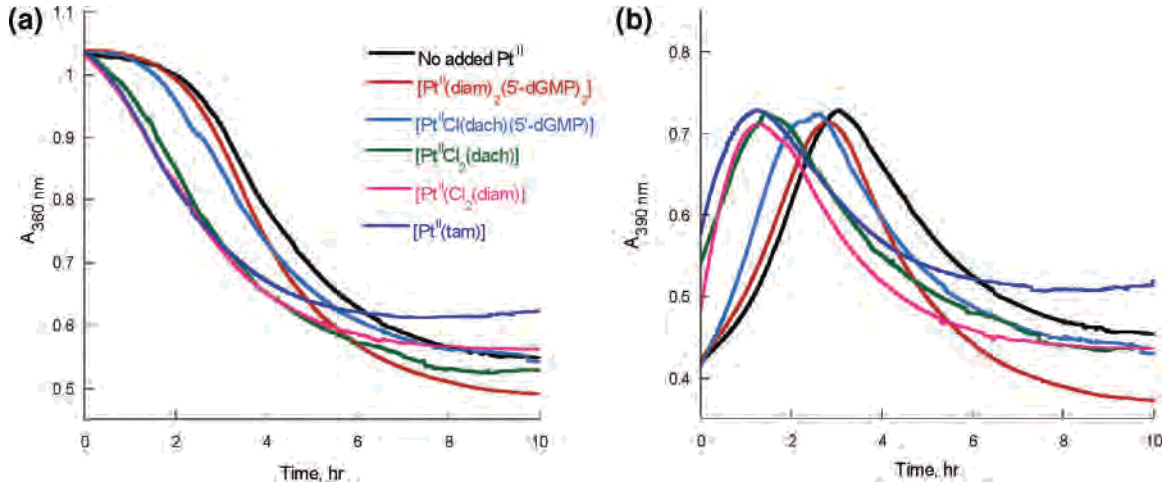

Figure 1. Absorbance at (a) 360 and (b) 390 nm vs time of 5 mM $[Pt^{IV}Cl_4(dach)]$ and 50 mM 5′-dGMP with 0.5 mM Pt^{II} complexes, pH 8.6 at 37 °C.

Chart 1. Structures of the Guanine Derivatives and Platinum Complexes Studied

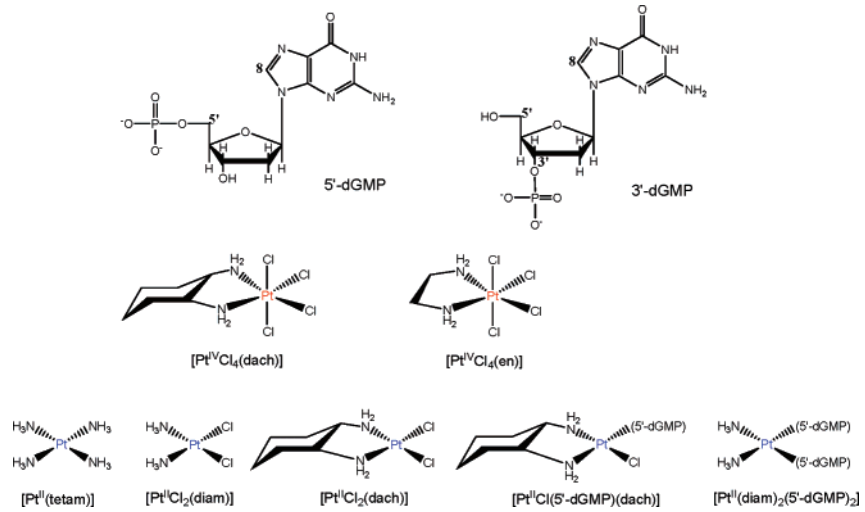

(0.5 mL/min) conditions with a solvent of 0.5% formic acid in water. An ion-trap mass spectrometer was to select for specific masses used with fragmentation both on and off. The MS parameters were set to scan from 50 to 2200 *m/z* using positive detection with electrospray ionization mass spectrometry (ESI-MS). For tuning, the nebulizer was set to 50 psi, the dry gas flow to 9 L/min, and the dry temperature to 365 °C.

Kinetic Studies. Appropriate amounts of 3′- or 5′-dGMP were added to vials containing equal volumes of platinum stock and saline solutions to achieve the desired dGMP concentrations. The pH values of the solutions were adjusted to pH 8.3 with NaOH using a pH meter (Orion Research 960) equipped with a Mettler-Toledo Inlab combination pH microelectrode. Attainment of the desired pH constituted the beginning of the reaction. UV−vis spectra were obtained in 10 mm cells on a Varian Cary 4000i spectrophotometer with Cary WinUV kinetic assay software. The absorbances at 360 and 390 nm were monitored. The sample temperature was maintained by a Varian-Cary temperature controller. Kinetic experiments were repeated at least three times.

Results and Discussion

Effect of Added Pt^{II} Complexes on the Reaction of $[Pt^{IV}Cl_4(dach)]$ and 5′-dGMP. Figure 1 compares the A_{360} and A_{390} versus the time of the reactions of $[Pt^{IV}Cl_4(dach)]$ and 5′-dGMP without and with added Pt^{II} complexes such as $[Pt^{II}Cl_2(dach)]$, $[Pt^{II}Cl(dach)(5'\text{-dGMP})]$, $[Pt^{II}Cl_2(diam)]$, $[Pt^{II}Cl(diam)(5'\text{-dGMP})_2]$, and $[Pt^{II}(tetam)]$. The absorbances at 360 and 390 nm are mainly from the initial $[Pt^{IV}Cl_4(dach)]$ and the intermediate $[Pt^{IV}Cl_3(dach)(5'\text{-dGMP})]$ ($[Pt^{IV}-G]$), respectively.[2a,b] Without added Pt^{II} catalysts, there is a long induction time for the reaction to start. All of the Pt^{II} complexes shorten the induction time (Figure 1a) and produce the $[Pt^{IV}-G]$ intermediate at an earlier time than when the reaction is run without a catalyst (Figure 1b). Without added Pt^{II}, the $[Pt^{IV}-G]$ intermediate reached maximum concentration at around 3 h, but with the addition of 10% (mol) $[Pt^{II}(diam)(5'\text{-dGMP})_2]$, $[Pt^{II}Cl(dach)(5'\text{-dGMP})]$, $[Pt^{II}Cl_2(dach)]$, $[Pt^{II}Cl_2(diam)]$, and $[Pt^{II}(tetam)]$, it became 2.78, 2.52, 1.48, 1.28, and 1.27 h, respectively. The smallest catalysts, $[Pt^{II}(tetam)]$ and $[Pt^{II}Cl_2(diam)]$, are the most efficient, followed by $[Pt^{II}Cl_2(dach)]$, $[Pt^{II}Cl(dach)(5'\text{-dGMP})]$, and $[Pt^{II}(diam)(5'\text{-dGMP})_2]$ in order, coinciding with increasing ligand size.

Identification of Intermediate, $Pt^{IV}-G$. To further elucidate the substitution reaction, the $Pt^{IV}-G$ intermediates of the $[Pt^{IV}Cl_4(dach)]/5'$-dGMP reaction catalyzed by $[Pt^{II}$-

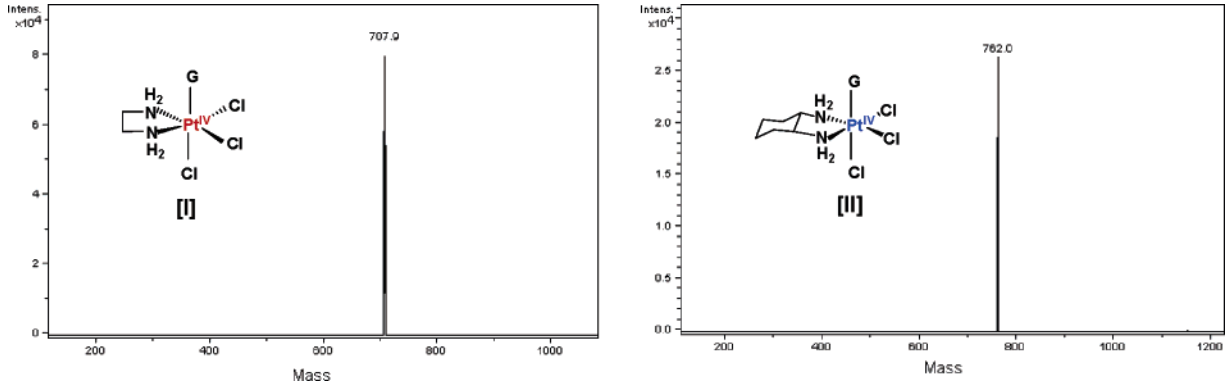

Figure 2. Mass spectra of [$Pt^{IV}Cl_3$(en)(5′-dGMP)] (**I**) and [$Pt^{IV}Cl_3$(dach)(5′-dGMP)] (**II**). The intermediate complex was acquired using the ion trap set for masses of (**I**) 708 and (**II**) 762 amu with no fragmentation from the reaction of [$Pt^{IV}Cl_4$(dach)]/[Pt^{II}(en)Cl_2]/5′-dGMP (1/0.7/10 mM). The [$Pt^{IV}Cl_4$(dach)]/[$Pt^{II}Cl_2$(dach)]/5′-dGMP (1/0.7/10 mM) reaction generates only **II**.

Scheme 2. Pt^{II}-Catalyzed Pt^{IV}-Substitution Reaction

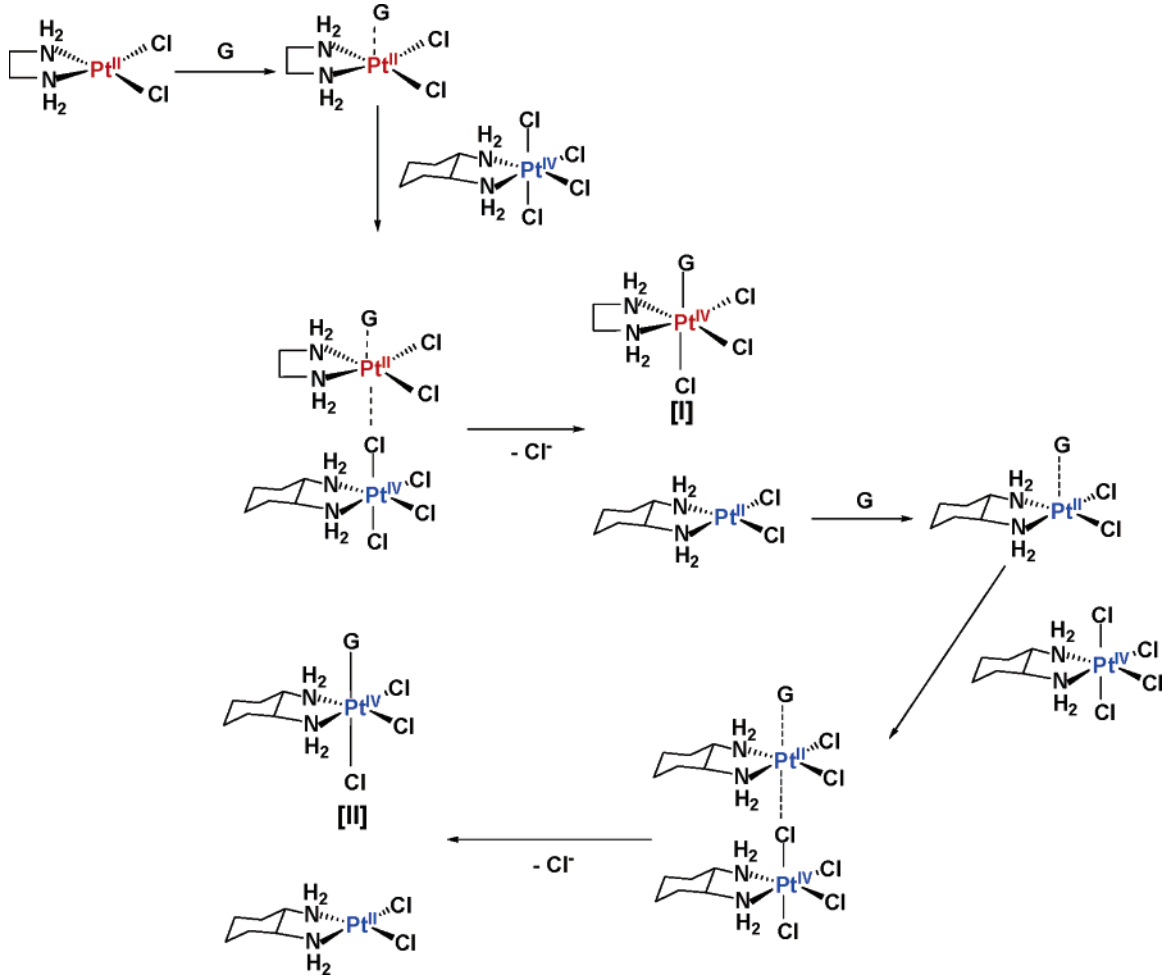

Cl_2(en)] and by [$Pt^{II}Cl_2$(dach)] were identified by LC/MS. The LC/MS was performed on each reaction when the intermediate concentration observed by A_{390} was maximum. Figure 2 displays the LC/MS spectra of the [$Pt^{IV}Cl_4$(dach)]/[$Pt^{II}Cl_2$(en)]/5′-dGMP reaction. It shows a 707.9 amu peak for [$Pt^{IV}Cl_3$(en)(5′-dGMP)] (**I**), as well as a 762.0 amu peak from [$Pt^{IV}Cl_3$(dach)(5′-dGMP)] (**II**). The LC/MS spectrum of the [$Pt^{IV}Cl_4$(dach)]/[$Pt^{II}Cl_2$(dach)]/5′-dGMP reaction only shows a 762 amu peak from [$Pt^{IV}Cl_3$(dach)(5′-dGMP)] (**II**). These results are best explained by consideration of the Basolo−Pearson Pt^{II}-catalyzed Pt^{IV}-substitution reaction where the central platinum is exchanged between the Pt^{II} catalyst and Pt^{IV} substrate (Scheme 2).[11] For the [$Pt^{IV}Cl_4$(dach)]/[Pt^{II}-Cl_2(en)]/5′-dGMP reaction, 5′-dGMP binds to $Pt^{II}Cl_2$(en) to produce 5-coordinate [$Pt^{II}Cl_2$(en)(5′-dGMP)], which then binds to [$Pt^{IV}Cl_4$(dach)] through a chloro ligand to form [Pt^{IV}-Cl_3(dach)Cl···$Pt^{II}Cl_2$(en)(5′-dGMP)]. Two electrons transfer

(11) (a) Basolo, F.; Wilks, P. H.; Pearson, R. G.; Wilkins, R. G. *J. Inorg. Nucl. Chem.* **1958**, *6*, 161. (b) Mason, W. R. **1972**, *7*, 241−255. (c) Summa, G. M.; Scott, B. A. *Inorg. Chem.* **1980**, *19*, 1079. (d) Cox, L. T.; Collins, S. B.; Martin, D. S. *J. Inorg. Nucl. Chem.* **1961**, *17*, 383.

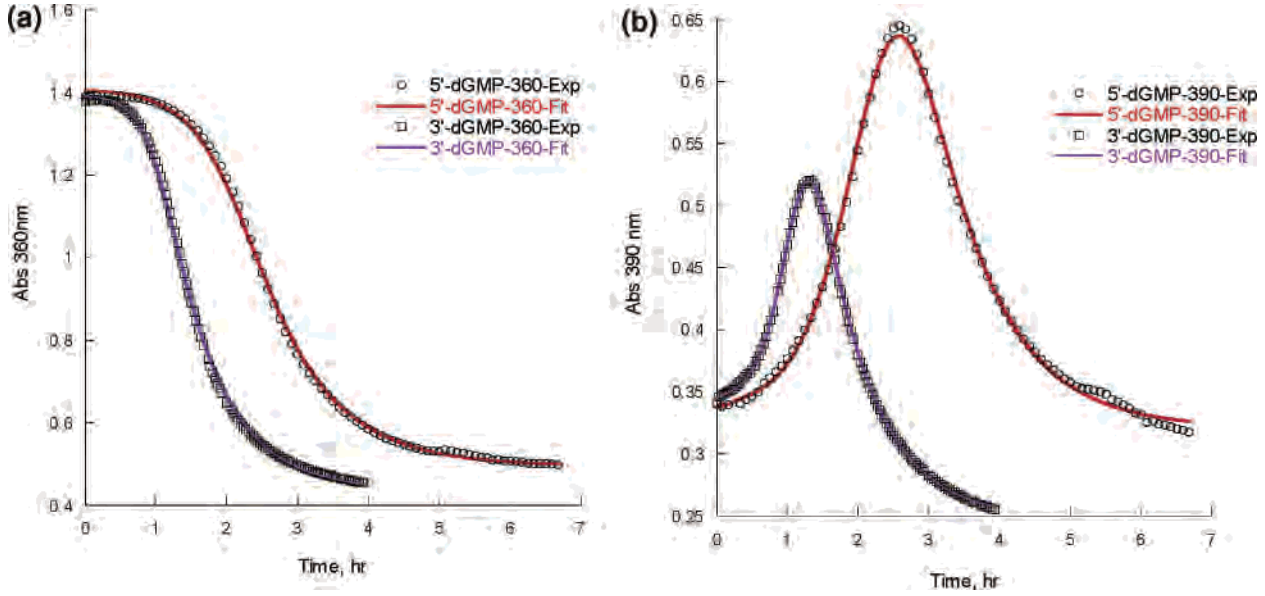

Figure 3. (a) A_{360} and (b) A_{390} vs time of 5 mM [$Pt^{IV}Cl_4$(dach)] with 50 mM 5′- and 3′-dGMP reactions in 100 mM NaCl, pH 8.3 at 40 °C. Both fits give $k_s = 20.4\ M^{-2}\ s^{-1}$ and $k_e = 3.9 \times 10^{-4}\ s^{-1}$ for 3′-dGMP and $k_s = 8.1\ M^{-2}\ s^{-1}$ and $k_e = 3.6 \times 10^{-4}\ s^{-1}$ for 5′-dGMP.

Scheme 3. Kinetic Model for the Oxidation of G by [PtIVCl4(dach)]

$$Pt^{IV}\text{–}Cl + G + Pt^{II} \xrightarrow{k_s} Pt^{IV}\text{–}G + Pt^{II} \quad (1)$$

$$Pt^{IV}\text{–}G \xrightarrow{k_e} Pt^{II} + G\,(-2e) \quad (2)$$

from Pt^{II} to Pt^{IV} through chloride ligand to generate [$Pt^{II}Cl_2$(dach)] and [$Pt^{IV}Cl_3$(en)(5′-dGMP)]. In the subsequent reaction, 5′-dGMP binds to [$Pt^{II}Cl_2$(dach)] to produce 5-coordinate [$Pt^{II}Cl_2$(dach)(5′-dGMP)], which then binds to [$Pt^{IV}Cl_4$(dach)] through a chloro ligand to form [$Pt^{IV}Cl_3$(dach)Cl···$Pt^{II}Cl_2$(dach)(5′-dGMP)]. Two electrons transfer from Pt^{II} to Pt^{IV} through a chloride ligand to generate [$Pt^{II}Cl_2$(dach)] and [$Pt^{IV}Cl_3$(dach)(5′-dGMP)].

Kinetic Data Analysis of 3′- and 5′-dGMP Reactions with [$Pt^{IV}Cl_4$(dach)]. The time courses of 5 mM [$Pt^{IV}Cl_4$(dach)] reactions with 50 mM 5′- or 3′-dGMP at 40 °C are displayed in Figure 3. The A_{360} curve of 3′-dGMP has a much shorter induction time than 5′-dGMP, and the A_{390} curve shows that the intermediate [Pt^{IV}−3′-dGMP] reaches a maximum faster than [Pt^{IV}−5′-dGMP] (3 vs 1 h). The kinetic curves are sigmoidal shaped indicating autocatalysis. The mechanism shown in Scheme 1 is a combination of a substitution reaction and an inner-sphere electron-transfer reaction. As demonstrated by the identity of the Pt^{IV}−G intermediate (Figure 2), the substitution follows the Basolo−Pearson Pt^{II}-catalyzed Pt^{IV} substitution mechanism, and therefore the overall substitution reaction can be written as eq 1 in Scheme 3.[11] Even if no external Pt^{II} is added, a small amount is assumed to be present as an impurity.

The A_{360} and A_{390} vs time kinetic curves were processed by the DynaFit Software[8] using the kinetic model in Scheme 3. Figure 3 shows the close agreement between the experimental and modeled absorbance versus time. The data fit best when the initial Pt^{II} concentration was fixed at 0.4% of that of Pt^{IV}. We assume that [$Pt^{IV}Cl_4$(dach)] contained 0.4% of [$Pt^{II}Cl_2$(dach)] as an impurity.

Rate constants determined over a temperature range of 30−45 °C are reported in Table 1. The activation parameters, $\Delta H^{\ddagger}$ and $\Delta S^{\ddagger}$, calculated from a linear least-squares fit to plots of ln(k/T) versus $1/T$ (Figure 4) are also reported in Table 1.

The substitution rate of 3′-dGMP is approximately twice as fast as that of 5′-dGMP at temperatures between 30 and 45 °C ($k_s^{35} = 14.8$ and 7.1 $M^{-2}\ s^{-1}$, respectively). The $\Delta H_s^{\ddagger}$ of 3′-dGMP is approximately 70% bigger than that of 5′-dGMP (50.4 and 30.7 kJ mol^{-1}, respectively). The enthalpic stabilization of 5′-dGMP may be caused by the hydrogen bonding between the 5′-phosphate and the NH of the (dach) ligand.[10] The 3′-phosphate is too far away to participate in hydrogen bonding with the NH of the ligand. The $\Delta S_s^{\ddagger}$ of 3′-dGMP is significantly bigger than that of 5′-dGMP (−59.4 and −129.5 J K^{-1} mol^{-1}, respectively), indicating that steric hindrance plays a major role in the substitution. The 5′-hydroxyl group exerts less steric hindrance than the 5′-phosphate group when the G binds to N7 (Chart 2). Dependence of a substitution on the steric hindrance of a carrier ligand has been well characterized by many researchers.[5]

3′-dGMP transfers electrons approximately twice as fast as 5′-dGMP at 35 °C (2.2×10^{-4} and $1.4 \times 10^{-4}\ s^{-1}$, respectively), but it is slightly slower at 45 °C (5.5×10^{-4} and $8.1 \times 10^{-4}\ s^{-1}$, respectively). The $\Delta H_e^{\ddagger}$ of 3′-dGMP is smaller than that of 5′-dGMP (88.8 and 137.8 kJ mol^{-1}, respectively). The $\Delta S_e^{\ddagger}$ of 3′-dGMP is much lower than that of 5′-dGMP (−27.8 and +128.8 J K^{-1} mol^{-1}, respectively). At low temperature, $\Delta H_e^{\ddagger}$ plays a major role in determining the rate constant. To initiate electron transfer, the nucleophilic group at the 5′-position should rotate to attack C8 as shown in Scheme 4. The lower $\Delta H_e^{\ddagger}$ of 3′-dGMP indicates that the 5′-hydroxo group in 3′-dGMP has a lower rotational barrier than the 5′-phosphate in 5′-dGMP. The lower rotational

Table 1. Rate Constants and Activation Parameters for Reactions of $[Pt^{IV}Cl_4(dach)]$ with 5′-dGMP and 3′-dGMP[a]

	k_s (M^{-2} s^{-1})					
	30 °C	35 °C	40 °C	45 °C	$\Delta H_s^{\ddagger}$ (kJ mol^{-1})	$\Delta S_s^{\ddagger}$ (J K^{-1} mol^{-1})
3′-dGMP	10.3 ± 0.3	14.8 ± 0.6	20.4 ± 0.5	27.9 ± 1.5	50.4 ± 0.9	−59.4 ± 1.3
5′-dGMP	5.4 ± 0.4	7.1 ± 0.2	8.1 ± 0.2	10.4 ± 0.2	30.7 ± 2.8	−129.5 ± 16.8
	k_e ($\times 10^4$ s^{-1})					
	30 °C	35 °C	40 °C	45 °C	$\Delta H_e^{\ddagger}$ (kJ mol^{-1})	$\Delta S_e^{\ddagger}$ (J K^{-1} mol^{-1})
3′-dGMP	1.0 ± 0.02	2.2 ± 0.1	3.9 ± 0.06	5.5 ± 0.3	88.8 ± 9.5	−27.8 ± 5.0
5′-dGMP	0.6 ± 0.1	1.4 ± 0.04	3.6 ± 0.5	8.1 ± 0.2	137.8 ± 2.9	+128.8 ± 3.6

[a] $[Pt^{IV}]$ = 5 mM, $[Pt^{II}]$ = 0.02 mM, and [dGMP] = 50 mM in 100 mM NaCl, pH 8.3.

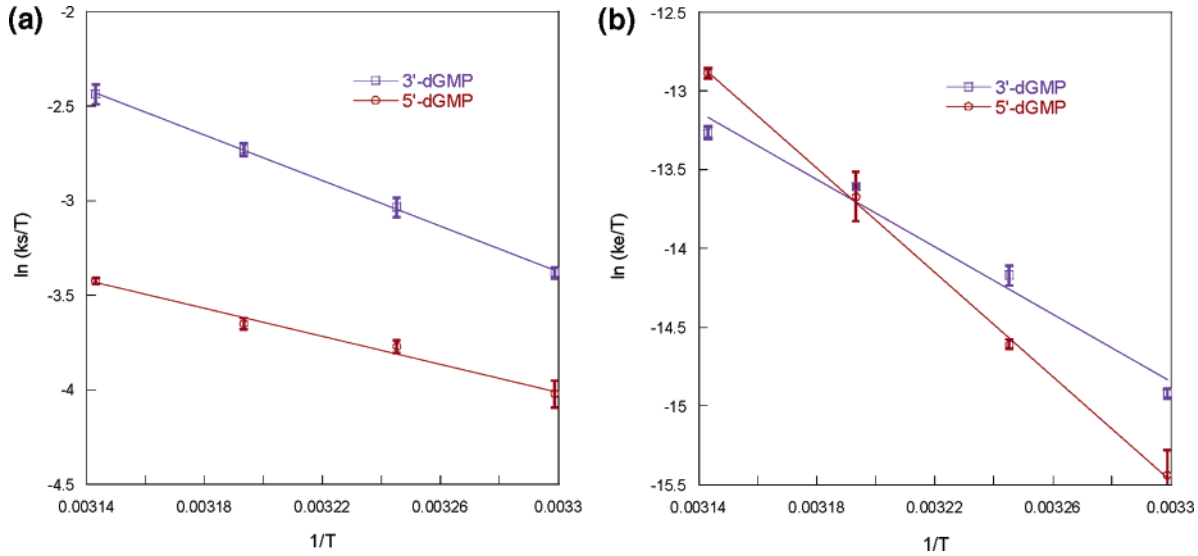

Figure 4. Plots of (a) $\ln(k_s/T)$ and (b) $\ln(k_e/T)$ vs $1/T$ for the reaction of 5 mM $[Pt^{IV}Cl_4(dach)]$ with 50 mM 5′-dGMP and 3′-dGMP.

Chart 2. Steric Hindrance between the dach Ligand and 5′- and 3′-dGMP

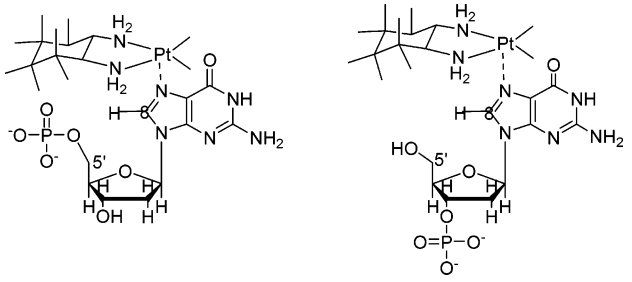

barrier of Pt−N for 3′-GMP than that for 5′-GMP is also reported by the Marzilli group.[12] But above 40 °C, $\Delta S_e^{\ddagger}$ plays a more important role. Cyclization and bond breaking are involved in the internal electron transfer: the former contributes a negative $\Delta S^{\ddagger}$ and the latter a positive $\Delta S^{\ddagger}$. Since the 5′-hydroxo group is much farther away from the C8 position than the 5′-phosphate group (Chart 2), 3′-dGMP must have a large negative $\Delta S^{\ddagger}$ of cyclization, which is not compensated by the positive $\Delta S^{\ddagger}$ of the bond breaking. However, since the 5′-phosphate in 5′-dGMP is close to C8,

(12) (a) Colonna, G.; Di Masi, N. G.; Marzilli, L. G.; Natile, G. *Inorg. Chem.* **2003**, *42*, 997−1005.(b) Carlone, M.; Fanizzi, F. P.; Intini, F. P.; Margiotta, N.; Larzilli, L. G.; Natile, G. *Inorg. Chem.* **2000**, *39*, 634−641. (c) Carlone, M.; Marzilli, L. G.; Natile, G. *Inorg. Chem.* **2004**, *43*, 584−592.

Scheme 4. Internal Electron Transfer through Cyclization

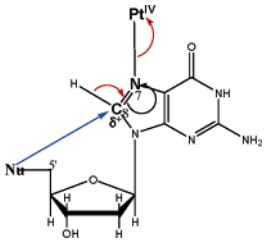

it may not have a large negative $\Delta S^{\ddagger}$ of cyclization, and the positive $\Delta S^{\ddagger}$ of bond breaking dominates in $\Delta S_e^{\ddagger}$, resulting in the positive $\Delta S_e^{\ddagger}$ value.

Comparison of $[Pt^{IV}Cl_4(en)]$ with $[Pt^{IV}Cl_4(dach)]$. The final G product of $[Pt^{IV}Cl_4(en)]$/5′-dGMP was the same as that of $[Pt^{IV}Cl_4(dach)]$/5′-dGMP, which was identified as 8-oxo-5′-dGMP by HPLC.[2a] The integration of the peaks reveals that the amount of 8-oxo-5′-dGMP generated by $[Pt^{IV}Cl_4(en)]$ was approximately 70% of the amount produced by $[Pt^{IV}Cl_4(dach)]$.

Figure 5 compares the time course of the A_{360} of the $[Pt^{IV}Cl_4(en)]$/$[Pt^{II}Cl_2(en)]$/5′-dGMP reactions with that of the $[Pt^{IV}Cl_4(dach)]$/$[Pt^{II}Cl_2(dach)]$/5′-dGMP reactions at 50 °C. It clearly shows that $[Pt^{IV}Cl_4(en)]$ reacts with 5′-dGMP in the same manner as $[Pt^{IV}Cl_4(dach)]$ but at a different rate. The k_s and k_e values of $[Pt^{IV}Cl_4(en)]$ obtained by fitting A_{360} to eqs 1 and 2 in Scheme 3 using DynaFit[8] are 25.2 M^{-2} s^{-1}

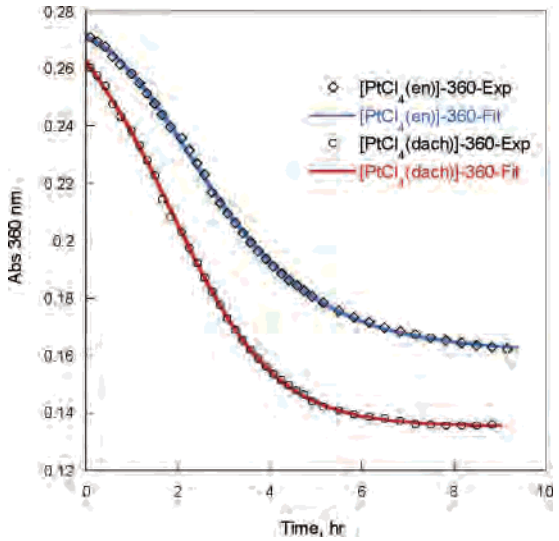

Figure 5. A_{360} vs time of $[Pt^{IV}Cl_4(en)]/[Pt^{II}Cl_2(en)]$ and $[Pt^{IV}Cl_4(dach)]/[Pt^{II}Cl_2(dach)]$ with 5′-dGMP reactions at 50 °C: $[Pt^{IV}] = 1$ mM, $[Pt^{II}] = 0.2$ mM, [5′-dGMP] = 20 mM, 100 mM NaCl, and pH 8.3. The solid lines are fit to eqs 1 and 2.

and 1.5×10^{-4} s^{-1}, respectively. The k_s and k_e values of $[Pt^{IV}Cl_4(dach)]$ are 11.1 M^{-2} s^{-1} and 14.2×10^{-4} s^{-1}, respectively. The results indicate that $[Pt^{IV}Cl_4(en)]$ is approximately twice as fast in substitution but approximately 10 times slower in electron transfer than $[Pt^{IV}Cl_4(dach)]$. The en ligand is a smaller carrier ligand than dach, which is responsible for the higher substitution rate of $[Pt^{IV}Cl_4(en)]$. But $[Pt^{IV}Cl_4(en)]$ has lower reduction potential ($E_c = -159 \pm 5$ mV vs Ag/AgCl) than $[Pt^{IV}Cl_4(dach)]$ ($E_c = -71 \pm 10$ mV vs Ag/AgCl), which explains the slow electron-transfer rate of $[Pt^{IV}Cl_4(en)]$.

Conclusion

We have compared the substitution rate constant (k_s) and the electron-transfer rate constant (k_e) in the redox reaction between Pt^{IV} and 3′-dGMP (or 5′-dGMP) using an autocatalytic kinetic model and DynaFit Software.[8] Activation parameters were obtained from the rate constants at temperatures between 30 and 45 °C. The results show that 3′-dGMP substitutes faster than 5′-dGMP because of its small steric hindrance. In the electron-transfer step, the reaction with 3′-dGMP is faster only at temperatures below 45 °C; the reaction with 3′-dGMP is enthalpically favorable, while the reaction with 5′-dGMP is entropically favorable. We have also shown that $[Pt^{IV}Cl_4(en)]$ is faster than $[Pt^{IV}Cl_4(dach)]$ in substitution because of its smaller carrier ligand but slower in electron transfer because of its low reduction potential. The results reported here contribute to our understanding of platinum anticancer drugs and DNA reactions, which may be important in the developement of new anticancer therapies.

Acknowledgment. This work was supported by the National Science Foundation (Grant CHE-0450060), the donors of Petroleum Research Fund administered by the American Chemical Society (Grant PRF-37873-B3), and the Vermont Genetics Network through the NIH Grant P20 RR16462 from the INBRE program of the National Center for Research Resources.

IC061243G